Coupling between electronic and lattice degrees of freedom in 4f-electron systems investigated by inelastic neutron scattering

2003 J. Phys.: Condens. Matter 15 S519

(http://iopscience.iop.org/0953-8984/15/5/307)

INSTITUTE OF PHYSICS PUBLISHING JOURNAL OF PHYSICS: CONDENSED MATTER

J. Phys.: Condens. Matter **15** (2003) S519–S536 PII: S0953-8984(03)55325-5

Coupling between electronic and lattice degrees of freedom in 4f-electron systems investigated by inelastic neutron scattering

M Loewenhaupt[1] **and U Witte**[2]

[1] Institut für Angewandte Physik (IAPD), TU Dresden, D-01062 Dresden, Germany
[2] Hahn-Meitner-Institut, Glienicker Str. 100, D-14109 Berlin, Germany

Received 29 October 2002
Published 27 January 2003
Online at stacks.iop.org/JPhysCM/15/S519

Abstract

In general, elementary excitations in solids such as crystal field (CF) transitions and phonons are considered decoupled and the determination and interpretation of the measured spectra of the two phenomena, i.e. the CF level schemes and the phonon dispersion relations, are performed independently of each other. In addition, the spectra of these two excitations are generally quite complex and hence any unusual features are difficult to detect. A signature of a strong coupling between the two phenomena is the observation of an unusual behaviour in both subsystems. To prove the coupling unambiguously it is therefore necessary to investigate e.g. the phonon dispersion relations of an isostructural compound where the magnetic rare-earth ion (Ce, Yb) is replaced by a non-magnetic, but chemically equivalent ion (Y, La, Lu) and to determine the CF schemes of the same compound with the rare-earth ion replaced by a 'normal' magnetic rare earth. This requires, of course, time-consuming, detailed investigations. With these considerations in mind, it is not a surprise that there are only a few examples known where a coupling between electronic (CF transitions) and lattice (phonons) degrees of freedom have been reported.

Here we will discuss results on three rare-earth compounds where the coupling between CF transitions and phonons has been unambiguously shown by inelastic neutron scattering experiments: $CeAl_2$, $YbPO_4$ and $CeCu_2$.

1. Introduction

Magnetic excitations in rare-earth (R) systems have been investigated intensively in the last few decades. The principal experimental method has been the inelastic neutron scattering technique. It turns out that the energy range over which the magnetic excitations occur is very well suited to neutron scattering investigation. There have also been investigations of the effect of crystal field (CF)–phonon coupling by Raman spectroscopy (for example [1, 2]).

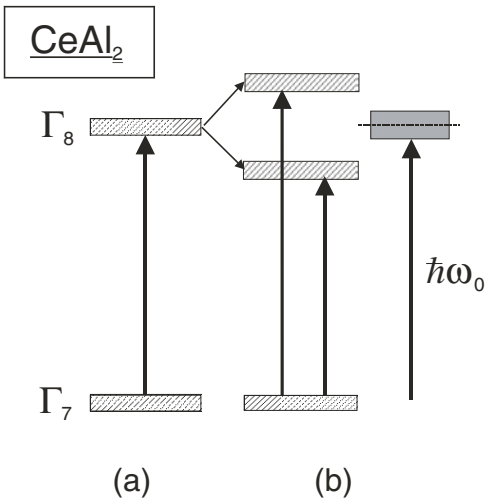

Figure 1. A schematic diagram for $CeAl_2$ of the expected (a) and the observed CF transitions (b). The grey region (right) corresponds to energies with high phonon density of states (from [5]).

In some cases it was found that the magnetic excitations are coupled to lattice degrees of freedom (phonons). Such interactions take place because a lattice deformation around an R ion modifies the crystalline electric field which is present at the R-ion site. This leads to anomalies in the phonon spectrum as well as to an unusual behaviour of the magnetic excitations.

In the following, three compounds will be discussed in which an unusual behaviour of CF transitions or phonons gave rise to more detailed investigations by inelastic neutron scattering.

The most pronounced effects have been observed in compounds containing Ce or Yb. Both ions have a Hund's rule ground state with a large orbital momentum ($L = 3$) and a small spin ($S = 1/2$, resulting from the one electron in Ce and the one hole in Yb in the 4f shell) yielding the values $J = 5/2$ and $7/2$ for the total angular momentum for Ce and Yb, respectively.

2. $CeAl_2$

The intermetallic compound $CeAl_2$ has a cubic Laves phase structure. From this, one expects for the $J = 5/2$ Hund's rule ground state multiplet of the Ce^{3+} ions a splitting due the crystalline electric field into a Γ_7 (doublet) and a Γ_8 (quartet) state connected by just one inelastic CF transition (see figure 1(a)). Neutron scattering experiments, however, revealed two inelastic magnetic transition lines [3] and, in addition, an unusual behaviour of the phonon spectrum with temperature [4]. A theoretical explanation of these findings was given by Thalmeier and Fulde [5], implying that in $CeAl_2$ a bound state between a CF excitation and phonons is formed (figure 1(b)). At this stage it was sufficient to treat the problem just locally, i.e. as a single-ion effect. Also the introduction of a phonon band yields the same, $\boldsymbol{Q}$-independent, double-peaked structure of the magnetic response [6]. However, the first inelastic neutron spectra already showed a detectable, though weak, $\boldsymbol{Q}$-dependence of the shape of the two-peak structure [3]. Therefore an improved theory which incorporates the wavevector and polarization dependence of phonon frequencies and coupling parameters would be desirable.

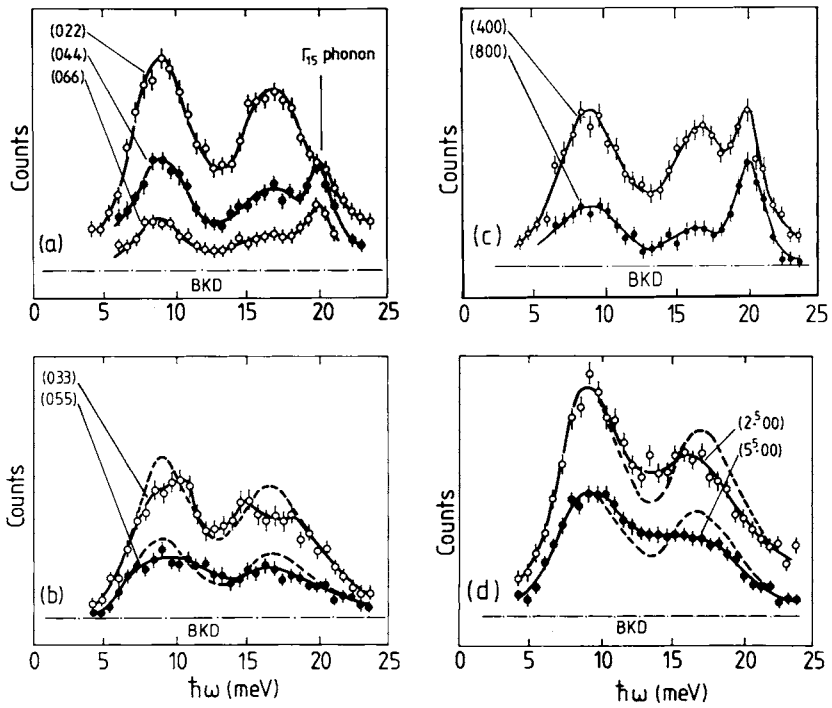

Figure 2. Inelastic neutron spectra of $CeAl_2$ at different reciprocal-lattice points taken on the neutron spectrometer IN8 at $T = 6$ K. The structure factor for the interacting phonon Γ'_{25} (around 10 meV) is zero for (a) and (c) and non-zero for (b) and (d). The non-interacting phonon Γ_{15} is indicated. BKD = background, assumed flat. The solid curve is only a guide to the eye. The dashed curve corresponds to simple two-peak structures as in (a) and (c) with intensity given by $F^2(\boldsymbol{Q})$ (from [7]).

2.1. Inelastic neutron experiments with unpolarized neutrons (IN8)

At temperatures $T = 6$ K, where $CeAl_2$ is in the magnetically disordered state above the antiferromagnetic ordering temperature of $T_N = 3.8$ K, the $\boldsymbol{Q}$-dependence of the two-peak structure was studied in detail [7].

For these experiments a large $CeAl_2$ single crystal with its (110) axis perpendicular to the scattering plane was used. Most of the spectra were taken on the high-intensity triple-axis spectrometer (TAS) IN8 (at the ILL Grenoble) in the constant-$\boldsymbol{Q}$ mode with unpolarized neutrons and in zero external field with fixed final neutron momentum k_f (3.8 $Å^{-1}$ corresponding to 30 meV) [8]. The spectra yield magnetic and phonon contributions to the scattering intensity. Figure 2 shows some of the spectra taken on IN8 at $T = 6$ K. Considering only the diamond structure of the Ce sublattice, there are the following equivalent Γ points: (220), (044), (066), (400) and (800).

At these points the spectra look very similar (figures 2(a), (c) and 3 (a)) and two well defined peaks at 9 and 17 meV are observable. Their widths (FWHM = 4 and 6 meV) are considerably larger than the experimental resolution (FWHM = 2 and 2.3 meV at the position of the first and the second peak, respectively). Their intensity decreases with increasing $\boldsymbol{Q}$-value according to the square of the magnetic form factor ($F(Q)$) of the Ce^{3+} ions. The sharp feature at 20 meV is due to the (non-coupling) Γ_{15} optical phonon [4]. Its intensity just adds to the magnetic intensity according to its structure factor times Q^2. The (coupling) phonon

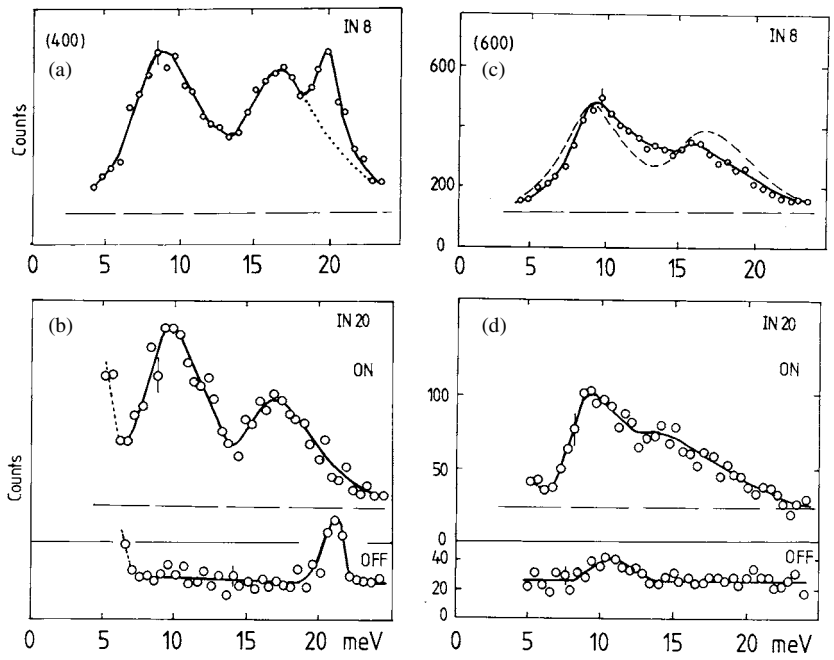

Figure 3. Inelastic neutron spectra of $CeAl_2$ at (004) and (006), which are non-equivalent points for the diamond Ce sublattice. Data taken at $T = 6$ K on the neutron spectrometers IN8 (unpolarized, (a) and (c)) and IN20 (polarized, (b) and (d)); typical measuring times per point are 10 and 14 min, respectively. In (b) the well defined magnetic double peak (ON, upper spectrum) and the non-interacting Γ_{15} phonon (OFF, lower spectrum) are visible. In (d) the 'deformed' magnetic response (ON, upper spectrum) and the broadened, interacting Γ'_{25} phonon (OFF, lower spectrum) can be seen. 'ON' means that the flipper is on (SF); magnetic scattering. 'OFF' means that the flipper is off (NSF); phonon scattering (from [7]).

Γ'_{25} has zero structure factor at the points discussed above. At all other points of the reciprocal lattice where the structure factor of the Γ'_{25} phonon is non-zero, much more complicated, 'deformed' spectra are observed. Some examples are shown in figures 2(b), (d) and 3(c). For comparison, the shape of the well defined two-peak structure as seen in figures 2(a), (c) and 3(a) is shown in the latter spectra as a dashed line with its intensity normalized by $F^2(Q)$. A clear deviation from the simple two-peak structure is obvious in these spectra. Before the analysis of these rather unusual spectra can proceed, the magnetic and phonon contributions to the total intensity have to be separated.

The only way to do this unambiguously is to use polarized neutrons and polarization analysis, available at the IN20 spectrometer (ILL Grenoble).

2.2. Inelastic neutron experiments with polarized neutrons and polarization analysis (IN20)

In these measurements, experimental configurations were used where the incident neutron polarization $\boldsymbol{P}_0$ was parallel to the momentum transfer $\boldsymbol{Q}$. In this case the scattering intensities are given by

$$I_u^{\mathrm{SF}} = \tfrac{2}{3} I_{\mathrm{inc}}^{\mathrm{spin}} + 0 + 0 + I_{\mathrm{magn}} + B^{\mathrm{SF}} \tag{1}$$

$$I_u^{\mathrm{NSF}} = \tfrac{1}{3} I_{\mathrm{inc}}^{\mathrm{spin}} + I_{\mathrm{inc}}^{\mathrm{isot}} + I_{\mathrm{coh}} + 0 + B^{\mathrm{NSF}}. \tag{2}$$

'SF' denotes scattering processes involving a (neutron) spin-flip; 'NSF' stands for non-spin-flip. For $CeAl_2$ the nuclear spin and isotope incoherent scattering intensities, $I_{\rm inc}^{\rm spin}$ and $I_{\rm inc}^{\rm isot}$, respectively, are negligibly small. Therefore, the purely magnetic scattering can be obtained directly when the flipper is ON (SF) and the phonon scattering when the flipper is OFF (NSF). B stands for background that may be different for SF and NSF cases.

As the IN20 measurements were performed with fixed incident neutron momentum $k_{\rm i}$ (4.1 Å^{-1} or 35 meV), instead of with fixed $k_{\rm f}$ as was the case for the IN8 measurements, different corrections should have been applied to the measured intensities. However, this was not done at that time. We therefore present only the uncorrected IN20 data in figure 3(b) with the well defined magnetic double peak (ON, upper spectrum) and non-interacting Γ_{15} phonon (OFF, lower spectrum) and in figure 3(d) with 'deformed' magnetic response (ON, upper spectrum) and broadened, interacting Γ'_{25} phonon (OFF, lower spectrum). These are compared to the spectra obtained with unpolarized neutrons (IN8) taken at the same reciprocal-lattice vectors. This comparison demonstrates that the unusual $\boldsymbol{Q}$-dependence of the double-peak structure is of magnetic origin.

2.3. Phonon dispersion relations

While the observed two-peak structure of the magnetic CF excitations was in striking contrast to the expected one-peak CF transition for Ce^{3+} ions in cubic symmetry and hence a strong indication of some anomalous behaviour of the magnetic properties of $CeAl_2$, it took considerably longer before it was experimentally proven that this was due to an extremely strong CF–phonon coupling. The proof required the investigation and analysis of the phonon dispersion relations for this type of crystal structure, the cubic Laves phase, with 18 phonon modes.

For this investigation, two large single crystals with volumes of several cm^3 were used. The first experiments were performed on the triple-axis spectrometer TAS1 at FR2 Karlsruhe at temperatures of 296, 80 and 5 K [4]. The results at 296 K are presented in figure 4. The full curves were calculated with a Born–von Karman model fitted to the experimental data. The broken curves indicate the slopes of the acoustic branches at the Γ point as calculated from the elastic constants [9]. The energy of the Γ'_{25} phonon (13.4 meV) is close to the average energy of the two-peak structure of the CF excitations with peaks at 9 and 17 meV ($26/2 = 13$ meV). Figure 5 gives a summary of the most important results at 5 K. The symbols represent the measured data at 5 K; the full and broken lines indicate the corresponding branches at room temperature and at 80 K, respectively.

For small phonon wavevectors the transverse acoustic branches are in agreement with the slopes calculated from the elastic constants. The elastic constant C_{44} decreases by about 20% between 296 and 5 K, corresponding to a 10% reduction in the phonon frequencies for the branches Δ_5 and Σ_3. For larger wavevectors the phonons soften much more: at the zone boundary the branch is lowered by about 30%.

Reichardt and Nücker [4] also observed a double-peak structure of the transverse acoustic phonon branch in the [ξ00] direction. Thus, apart from the strong shift of the phonon peak position from 13.4 meV at 296 K to 10.0 meV at 5 K, a considerable broadening of the peaks is observed. In contrast, the frequency of the (non-interacting) Γ_{15} mode near 20 meV is essentially independent of temperature. In this latter mode, the Ce and Al sublattices vibrate as rigid bodies against each other. The phonon dispersion curves of $CeAl_2$ at 296 K are similar to those of the related compounds $LaAl_2$ and YAl_2. But in these compounds no anomalous temperature dependence of the C_{44} elastic constant occurs [10]. Measurements on YAl_2 demonstrated that the acoustic and low optical phonon branches behave quite normally,

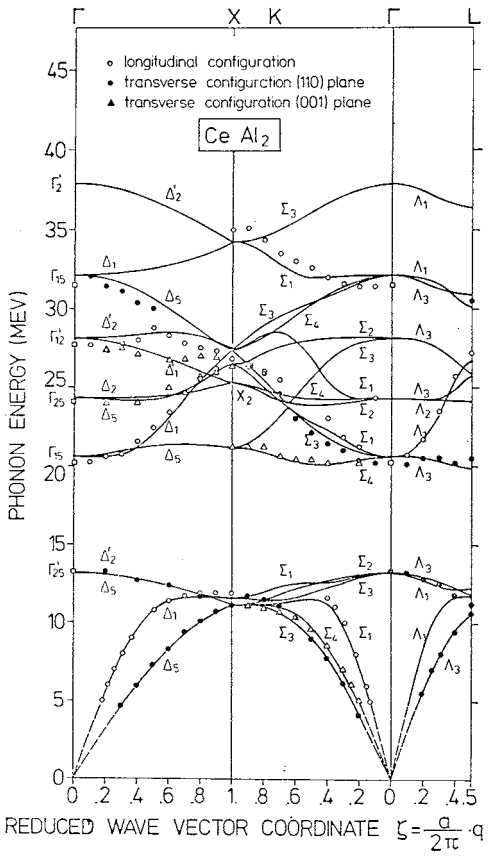

Figure 4. Phonon dispersion curves of $CeAl_2$ at 296 K. The solid curves were calculated with an axially symmetric Born–von Karman model. The broken curves indicate the slopes of the acoustic branches calculated from the elastic constants. The symbols give results for the longitudinal configuration (open circles), transverse configuration in the (110) plane (full circles) and transverse configuration in the (001) plane (triangles) (from [4]).

i.e., the phonon frequencies stiffen by a few parts per thousand between 296 and 5 K in all branches [11].

The pronounced phonon softening observed in $CeAl_2$ is assumed to be caused by a coupling of the lattice vibrations to the orbital moments R. It has been demonstrated by Cullen and Clark [12] that at $Q = 0$ this coupling occurs only for the Γ'_{25} lattice mode where the two Ce sublattices vibrate with opposite phases. This is in accordance with the observation that the Γ_{15} frequency is nearly independent of temperature. As the other optical modes, which have not been investigated in detail so far, also involve Al vibrations, no drastic temperature effects are expected there.

Two essential factors are responsible for the anomalous features in the CF excitations and the vibrational spectrum of $CeAl_2$:

(i) the near coincidence in energy of the CF excitation with flat optical branches of Γ'_{25} character; and

(ii) a very strong coupling between the (orbital) moment of the Ce ions and the lattice modes.

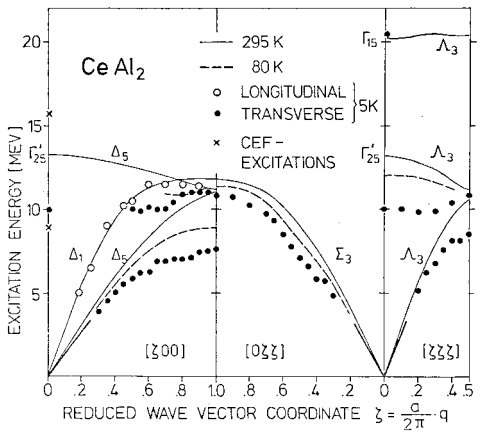

Figure 5. Phonon frequencies of selected branches in $CeAl_2$ at three different temperatures: 296 K (solid curves), 80 K (dashed curves) and 5 K (symbols, as in figure 4). The bold curves show the slopes of the TA branches (Δ_5, Σ_3, Λ_3) at 5 K calculated from the elastic constants. The crosses show the CF excitations (from [4]).

3. $YbPO_4$

$YbPO_4$ is an insulator with zircon structure yielding 36 phonon modes and a Hund's rule Yb^{3+} ($^2F_{7/2}$) ground state multiplet that is split by the low-symmetry CF into four doublets. Strong temperature effects on the CF spectra and damping of phonons lead to the presumption of an underlying mechanism involving monopolar fluctuations of the Yb 4f orbital [13].

The splitting of the f-electron energy levels belonging to R ions situated on specific crystallographic sites of a crystalline solid is well known. When the energy separations between the states within the Hund's rule ground multiplet are comparable with the energies of thermal and zero-point motion of the lattice, a coupling of the two subsystems may give rise to complex thermodynamic phenomena. The situation becomes simpler, in principle, for insulating materials, as mediation by conduction electrons can be ignored. A treatment of the ion–lattice interaction within the framework of cooperative Jahn–Teller (JT) effects points to either a setting in of a (static) lattice distortion at low temperature or continual (dynamic) fluctuations between energetically equivalent configurations of CF and phonon states [14, 15]. The former situation arises from a cooperative coupling of the electronic states to long-wavelength acoustic phonons (bulk strain modes) or optical phonons at the Brillouin zone centre and manifests itself in anomalous static properties such as structural changes, magnetostriction and softening of elastic moduli near the transition temperature (T_D). The latter situation is more complex. It depends on the matrix elements of the CF–phonon interaction, which in general depends on the phonon wavevector, and its manifestation relies on the energy-transfer mechanism in specific dynamic properties.

The CF–lattice interactions in a family of insulators RMO_4 (R = rare earths, M = P, V and As), which crystallize in the zircon structure (space group $I4_1/amd$), have been studied by many workers (for detailed citations, see e.g. [13]). Most of the observed JT effects relate to the static cooperative JT phase transition which involves a lattice distortion at low temperature. Evidence of dynamic JT effects in these materials, on the other hand, is expected to be less conspicuous as compared to the cases for static JT phase transitions or long-range magnetic ordering. In order to detect these effects, the dynamic properties have to be examined over a wide range of wavevectors and temperatures.

A candidate for use in studies of the dynamic nature of the JT effect is $YbPO_4$. Becker and co-workers [2] report the mixing of two Yb^{3+} CF states at 32 and 43 meV with an E_g phonon mode at 37 meV from 4.2 to 295 K from Raman scattering. Nipko and co-workers [16] report a ∼20% softening of the $(C_{11} - C_{12})/2$ elastic constant with temperature decreasing from 300 to 10 K, but there is no structural phase transition. The CF excitation spectra obtained from neutron time-of-flight spectroscopy using polycrystalline samples reveal broad and asymmetric CF peaks down to 10 K. The relative intensities of these CF transitions cannot be explained quantitatively by a single-ion CF model. Furthermore, the CF peaks become overdamped as soon as the temperature rises above ∼100 K.

For a quantitative characterization of the CF–lattice interactions in $YbPO_4$, inelastic neutron scattering experiments on single crystal were performed that were capable of differentiating the wavevector-dependent contributions. Additionally, phonon data from an isostructural, non-magnetic reference compound are needed for comparison. The latter were obtained by measuring the major phonon dispersion curves of $LuPO_4$ using neutron triple-axis spectroscopy [17].

The single crystals of $YbPO_4$ (∼0.5 cm^3) and $LuPO_4$ (∼0.75 cm^3) were grown using a flux technique. The neutron scattering experiments were performed using the 2T1 (now: 1T1) triple-axis spectrometer at the Laboratoire Leon Brillouin in Saclay, France. The ground state multiplet of Yb^{3+} ions in $YbPO_4$ with total angular momentum $J = 7/2$ is split into four Kramers doublets Γ_6, Γ_7, Γ_6 and Γ_7 at 0, 12, 32 and 43 meV, respectively [16]. They overlap with the acoustic and the first six optical phonon branches which are characterized by a substantial motion of the Yb ions. The measurements comprise a majority of these phonon branches as well as the CF transitions along the $[x00]$, $[xx0]$ and $[00x]$ symmetry directions at 20 and 295 K. Additional data were taken at 100, 180 and 475 K in order to examine the temperature dependence of the CF–phonon excitations.

A majority of the phonon energies of $YbPO_4$, as measured from reciprocal-lattice points that provide favourable intensities according to structure factor calculations, follow closely the corresponding phonon data for $LuPO_4$. There is no clear evidence of drastic phonon energy shifts, or splitting or softening of any phonon branches. However, in the 30–50 meV region, the phonon intensities are smeared by the superposition of two broad CF peaks around 32 and 43 meV that correspond to transitions from the ground state to the upper Γ_6 and Γ_7 CF states, respectively. If the CF–phonon interaction is small, the CF linewidths would be comparable to the instrumental resolution. This is the case for other RPO_4 (R = Tb to Tm) compounds [18, 19]. Since polarized neutrons were not employed in the measurements, the relative contributions from magnetic CF and nuclear (phonon) scattering intensity cannot be assigned accurately. Nevertheless, the magnetic intensities can be seen clearly from scans taken from reciprocal-lattice vectors where the phonon structure factors are small. Figures 6(a) and (b) show the energy scans for $YbPO_4$ and $LuPO_4$ at $\boldsymbol{Q} = (4.1\,0\,0)$ and (004), respectively. For $YbPO_4$ at 20 K, CF excitations from the ground state give rise to three peaks at 12, 32 and around 43 meV. The superimposed weak features of phonon origin can be seen from the corresponding spectra of $LuPO_4$. Normally, the observed intensity of a transition between two CF states is proportional to the (square of) the matrix element of the component of the angular momentum operator that is perpendicular to $\boldsymbol{Q}$ multiplied with the (square of) the magnetic form factor of the Yb^{3+} ion. Therefore, these scans permit a comparison of the data with the calculated intensity obtained from a single-ion CF model. Using the CF parameters as derived independently from a neutron experiment on a polycrystalline sample [16], one finds very good agreement between the observed anisotropic intensities and calculations. For example, at $T = 100$ K the ratios of the observed intensities between the (004) and $(4.1\,0\,0)$ scans (figure 6), after normalization according to the form-factor dependence, for the 12 and

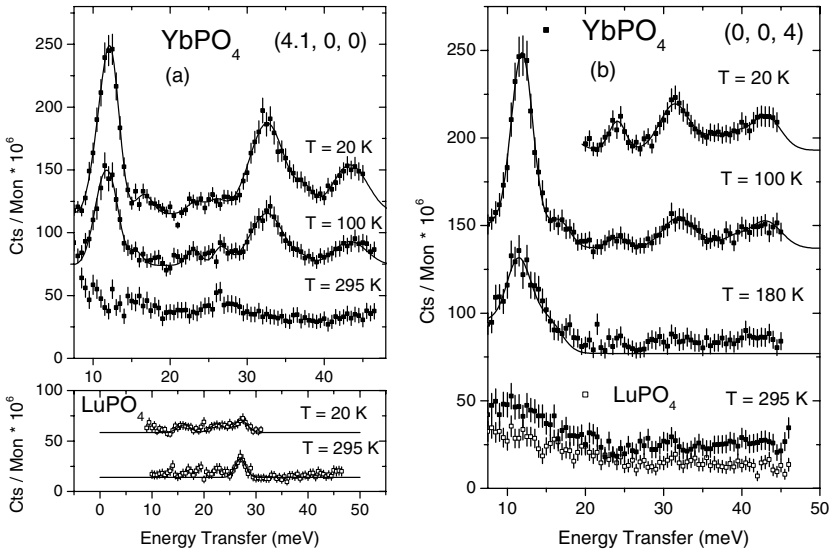

Figure 6. The excitation spectra of $YbPO_4$ and $LuPO_4$ at constant $\boldsymbol{Q}$: (a) $\boldsymbol{Q} = (4.1\,0\,0)$ and (b) $\boldsymbol{Q} = (004)$. The $LuPO_4$ data show the phonon background for comparison. For clarity, each data set was shifted vertically by a constant interval. A sharp peak centred at 12 meV was observed at 20 K at (004) in a separate scan but was not shown here in (b) (from [13]).

32 meV peaks are 1.96 ± 0.2 and 0.518 ± 0.06, respectively. The ratios of the corresponding matrix elements are 2.0 and 0.502. Therefore, in a $(\boldsymbol{Q}, T)$ region where CF transitions do not interfere with phonons, the magnetic intensity can be described by a single-ion CF model.

In spite of the qualitative agreement between the CF data and model calculations, there are a number of peculiarities. First, the CF lines, particularly the 32 and 43 meV peaks, are unusually broad. Second, the profile of the 32 meV peak is highly asymmetric. Third, all the CF transitions damp out upon increasing temperature much more rapidly than the expected behaviour based on the population factor of four CF lines. Fourth, the origin of a small peak at around 24 meV (figure 6(b)) is not understood. In general, these CF characteristics except for the extra peak at 24 meV were observed throughout the reciprocal space.

The CF–phonon interaction was investigated through taking extensive energy scans at many $\boldsymbol{Q}$-vectors guided by the 'bare-phonon' intensities estimated from the $LuPO_4$ data and a lattice dynamics shell model [17]. The most intense CF–phonon coupling occurs in the 30–50 meV region where phonons in $YbPO_4$ are strongly renormalized by CF excitations. Figures 7(a) and (b) show the constant-$\boldsymbol{Q}$ scans at (510) over a wide range of energies and temperatures for $YbPO_4$ and $LuPO_4$. At low energies (figure 7(a)), a phonon at 15.5 meV at 20 K (15.8 meV at 295 K) is clearly seen in $LuPO_4$. While its intensity increases according to the Bose–Einstein statistics, the slight increase in energy with increasing temperature is unexpected. This phonon and a similar energy shift are also observed in $YbPO_4$. In addition, the CF peak at 12 meV is clearly evident in $YbPO_4$ at 20 K, and it quickly broadens and dissipates at higher temperatures. However, the CF peak does not affect the intensity or the line shape of the phonon. At high energies (figure 7(b)) the $LuPO_4$ scans show two strong phonons at approximately 23 and 39 meV as well as weak ones around 19, 24 and 45 meV. In $YbPO_4$ the phonons below 30 meV, which do not overlap with any CF excitations from the ground state, resemble closely to those of $LuPO_4$. Above 30 meV the spectrum at 20 K is dominated by two broad CF peaks around 32 and 45 meV. The phonon at 39 meV is either

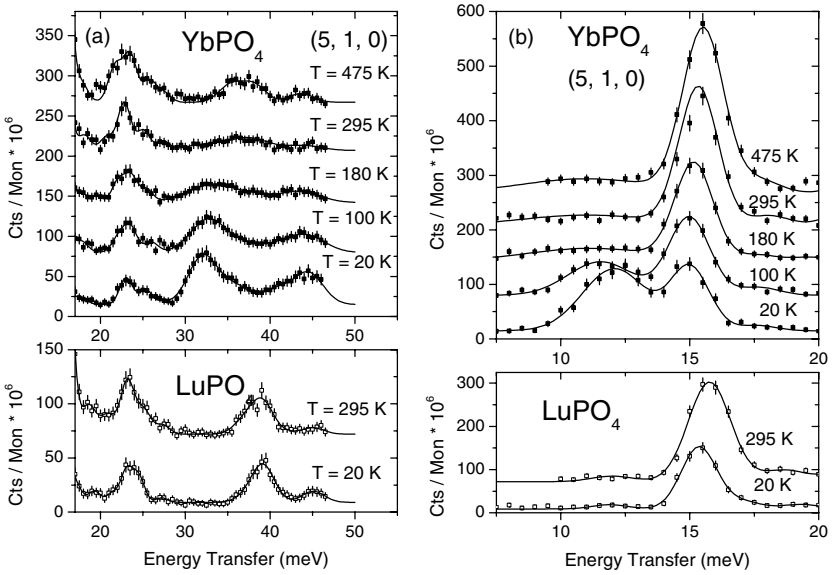

Figure 7. Constant-$\boldsymbol{Q}$ scans for $YbPO_4$ and $LuPO_4$ at selected temperatures in the (a) high- and (b) low-energy regions. For clarity, each data set was shifted vertically by a constant interval (from [13]).

suppressed, or shifted to 35.2 meV and mixed with the CF peak at 32 meV. The CF peaks broaden and weaken to the extent of being almost unrecognizable at 180 K, and at the same time, a gradual recovery of the phonon intensities centred around 37 meV can be seen as temperature increases. At 475 K two broad phonon peaks are seen similar to those for $LuPO_4$ but at slightly lower energies.

The neutron experiment discussed provides clear evidence of CF–lattice interactions in $YbPO_4$ that are unique among the RPO_4 family. Although the Yb^{3+}:$^2F_{7/2}$ ground multiplet splits into four Kramers doublets of Γ_6 (0 meV), Γ_7 (12 meV), Γ_6 ($\sim$32 meV) and Γ_7 ($\sim$43 meV) following the point symmetry at the R site, the anomalous CF linewidths and transition strengths clearly indicate energy-transfer processes between the magnetic ions and the host lattice. First, any further splitting of the Kramers doublets would require the breaking of time-reversal symmetry, such as from an electromagnetic field, rather than by local or global structural distortions. The present results of severe broadening and hints of splitting (figures 6 and 7) of the Kramers doublets confirm the dynamic nature of the CF–lattice interactions from 15 K to ambient temperature. Second, an interpretation of the evolution of mixed CF and phonon intensities in the 30–50 meV region would require a full diagonalization of a Hamiltonian properly including the magnetic and crystal lattices and their interactions. Third, coupling of the upper Γ_6 and Γ_7 CF states with phonons occurs over the entire Brillouin zone rather than involving phonons of specific symmetries. The interactions are strongest in the 200–400 K temperature range because of the relatively high CF energies.

The strong CF–lattice interactions in $YbPO_4$ indicate the presence of a fluctuating component associated with the Yb^{3+} ions. On the basis of the above observations and a multipolar expansion of the 4f orbitals, we may explore the nature of the fluctuations relevant to CF–phonon coupling in $YbPO_4$ following previous arguments used by Yamada [20] and Sinha [21]. In general, coupling of the anisotropic quadrupole moment of the low-lying CF states with certain symmetry-compatible stain modes (phonons in the long-wavelength limit) usually results in magnetostrictive effects. In the extreme case, the freezing out of

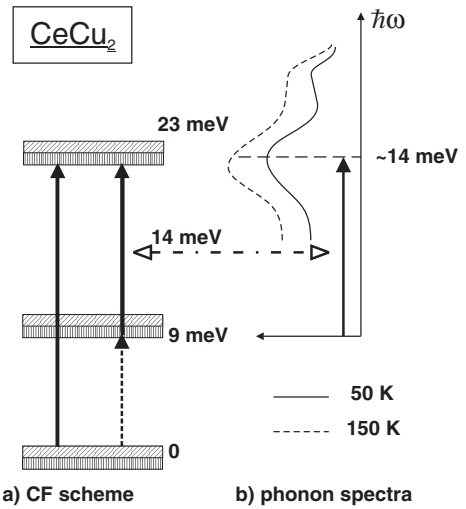

Figure 8. A schematic diagram for $CeCu_2$ of the CF level scheme (a) and of the phonon spectra (b) (from [23]).

the coupled CF strain modes at low temperatures may induce a static cooperative JT phase transition. In $YbPO_4$, however, except for a small ($\sim$20%) softening of the $(C_{11} - C_{12})$ elastic constants, neither magnetostriction nor lattice distortion was observed. Therefore, the quadrupole moment of Yb^{3+} ions in $YbPO_4$ is quite stable. Instead, the data suggest a large fluctuating component associated with the monopole term whereby coupling of the CF states, particularly the upper Γ_6 and Γ_7 doublets, with phonons occurs throughout the Brillouin zone. This feature is unique to all the RMO_4 compounds of zircon structure studied thus far.

4. $CeCu_2$

$CeCu_2$ is a Kondo lattice with antiferromagnetic order below 3.5 K and a Kondo temperature of about 6 K. It crystallizes in the orthorhombic $CeCu_2$ structure giving rise to 18 phonon modes. The $J = 5/2$ Hund's rule ground state of Ce^{3+} is split by the CF into three doublets yielding typically one weak and two strong inelastic transitions (the point symmetry at the Ce ion is C_{2v}).

From inelastic neutron scattering experiments (temperature-dependent time-of-flight measurements on polycrystalline samples) a CF level scheme was deduced: it has excited levels at 9 and 23 meV above the ground state [22] with a weak and a strong transition from the ground state to the first and second excited state, respectively, and a strong transition between the two excited states (see figure 8(a)).

In the temperature region between 100 and 150 K, where the anomalies in $CeCu_2$ have been observed, the first excited CF level becomes thermally populated. This has led to the assumption that there is a coupling between phonons and the CF transition from the first (9 meV) to the second (23 meV) excited level [23] (figure 8).

4.1. Inelastic neutron experiments with unpolarized neutrons (1T1)

Inelastic neutron scattering experiments were performed at the thermal triple-axis spectrometer 1T1 of the LLB in Saclay. A $CeCu_2$ single crystal of high quality grown at the Charles University in Prague was used [24].

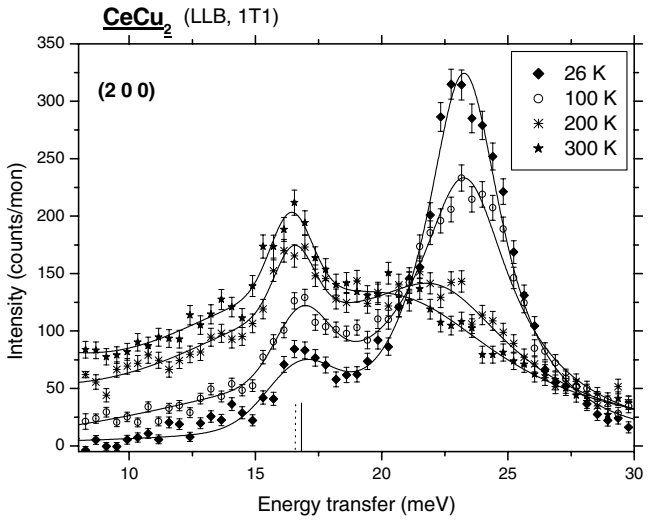

Figure 9. Inelastic neutron spectra of $CeCu_2$ at different temperatures for scattering vector $Q = (200)$ (data corrected for background). In the energy region below 20 meV an increase of intensity with temperature is visible, which arises from the intense, but extremely broadened 14 meV CF transition from the first to the second excited level. The longitudinal polarized phonon at 17 meV follows the normal temperature dependence of phonons. The solid curves perpendicular to the x-axis show the phonon position measured at 26 K, the dotted curves that at 300 K. At 23 meV the strong CF transition from the ground state to the second excited state is observed.

Neutron spectra were measured at different temperatures between 26 and 300 K (in the magnetically disordered state) with a fixed final neutron momentum k_f (2.66 $Å^{-1}$ or 14.7 meV) and an experimental resolution in energy between 0.2 and 0.6 meV for energy transfers between 5 and 25 meV, respectively.

The inelastic intensity observed in the neutron spectra has two different origins: magnetic scattering (from the CF transitions) and scattering due to the phonons.

In figures 9–11 the inelastic neutron spectra at $\boldsymbol{Q} = (200), (040)$ and $(0.7\,4\,0)$, respectively, are shown. In each figure the spectra measured at four different temperatures can be seen. To discuss the magnetic contribution to the total scattering intensity we first concentrate on figure 9, as there is only one phonon peak (at 17 meV) present.

The magnetic part of the observed spectrum at $T = 26$ K shows one intense, broad peak at 23 meV, which arises from the CF transition from the ground state to the second excited level. The other CF transition from the ground state to the first excited state at around 9 meV is not visible because of its negligible matrix element. As expected, the intensity of the 23 meV peak diminishes with increasing temperature because of the decreasing probability of that transition with rising temperature. Above 100 K, when the first excited CF level gets thermally populated, the 14 meV transition should become observable. However, the expected strong transition at 14 meV between the two excited levels is not observed as a distinct sharp peak at elevated temperatures. Instead, there is a strong rise of intensity in the whole energy region below 20 meV reminiscent of the 14 meV CF transition, which must be strongly broadened. This broadening is assumed to be due to the coupling of that CF transition and certain phonons in the energy range below 20 meV. To determine unambiguously the purely magnetic part of the spectrum, an investigation with polarized neutrons and subsequent polarization analysis was performed on IN20 recently. This will be discussed at the end of this section.

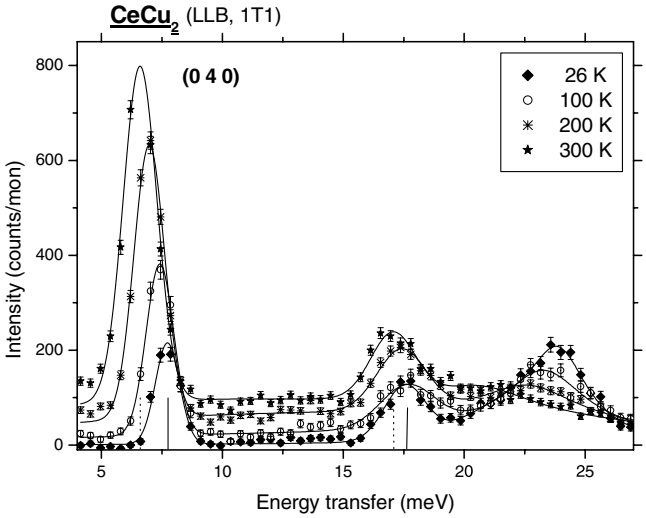

Figure 10. Inelastic neutron spectra of $CeCu_2$ at different temperatures for scattering vector $\boldsymbol{Q} = (040)$ (data corrected for background). The phonons at 17.5 and 7 meV both belong to another symmetry (A_{1g}) to the phonon shown in figure 9. They become unusually soft (shifted to lower energies) with increasing temperatures. The solid curves perpendicular to the x-axis show the phonon positions measured at 26 K, the dotted curves those at 300 K. At 23 meV the strong CF transition from the ground state to the second excited state is observed.

Coming back to the 1T1 experiments, a large number of inelastic scans were taken to search for anomalous behaviour in the phonon system. We found some phonon branches that became unusually soft (shifting to lower energies) with increasing temperature while other phonons showed the normal behaviour with temperature, i.e. a negligible shift. The phonons at 7 and at 17.5 meV (figure 10) as well as the phonon at 14 meV (figure 11) are shifting to lower energies much more strongly than expected for the normal temperature dependence of the phonon energy. In contrast, the phonons at 17 meV (figure 9) and at 8 meV (figure 11) show the normal behaviour. Furthermore, it was found that the behaviour, whether normal or unusual, depends on the symmetry of the phonon: all phonons with unusual behaviour belong to the same irreducible representation (A_{1g} symmetry of the phonons).

The strongest shift for a phonon peak was found at around 7 meV measured at $\boldsymbol{Q} = (040)$. Its energy at 300 K is lower by about 15% with respect to its energy at low temperature (26 K). Additionally, the linewidths of the shifted phonons strongly increase with temperature.

4.2. Inelastic neutron scattering with polarized neutrons and polarization analysis (IN20)

To prove the assumption that the increased intensity in the energy region below 20 meV at elevated temperatures above 100 K originates from magnetic scattering and not from other processes such as multiphonon scattering, it was necessary to separate the magnetic from the phonon intensity.

The same $CeCu_2$ single crystal as was used in the measurements on 1T1 was investigated on IN20 at different temperatures between 20 and 400 K and at selected $\boldsymbol{Q}$-values with a fixed final momentum of the neutrons of $k_f = 4.1$ Å^{-1} (equivalent to 35 meV) [25].

The experimental set-up of IN20 allowed not only the separation of magnetic and phonon scattering but also the determination of different components of the magnetic scattering as displayed in equations (3)–(8).

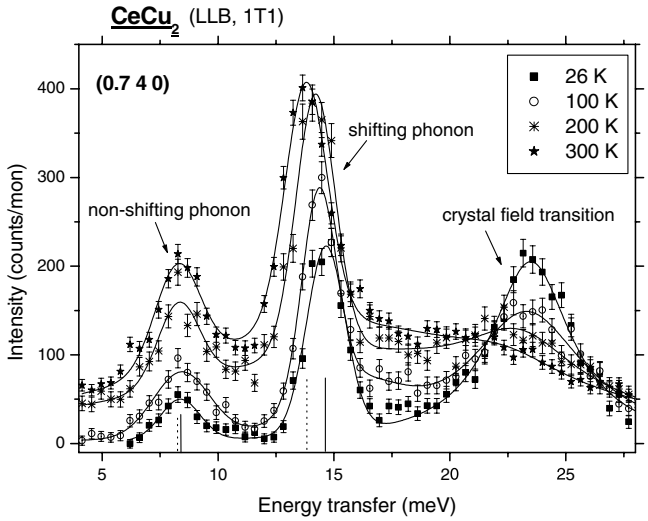

Figure 11. Inelastic neutron spectra of $CeCu_2$ at different temperatures for scattering vector $\boldsymbol{Q} = (0.7\,4\,0)$ (data corrected for background). The phonon at 14 meV has A_{1g} symmetry and becomes unusually soft (shifted to lower energies) with increasing temperature. The phonon at 8 meV has another symmetry and shows normal temperature behaviour. The solid curves perpendicular to the x-axis show the phonon positions measured at 26 K, the dotted curves those at 300 K. At 23 meV the strong CF transition from the ground state to the second excited state is observed.

For $\boldsymbol{P} \parallel \boldsymbol{Q}$:

$$I_u^{\mathrm{SF}} = \tfrac{2}{3} I_{\mathrm{inc}}^{\mathrm{spin}} + 0 + 0 + I_{\mathrm{magn}}^{v} + I_{\mathrm{magn}}^{w} \tag{3}$$

$$I_u^{\mathrm{NSF}} = \tfrac{1}{3} I_{\mathrm{inc}}^{\mathrm{spin}} + I_{\mathrm{inc}}^{\mathrm{isot}} + I_{\mathrm{coh}} + 0. \tag{4}$$

For $\boldsymbol{P} \perp \boldsymbol{Q}$:

$$I_v^{\mathrm{SF}} = \tfrac{2}{3} I_{\mathrm{inc}}^{\mathrm{spin}} + 0 + 0 + I_{\mathrm{magn}}^{w} \tag{5}$$

$$I_v^{\mathrm{NSF}} = \tfrac{1}{3} I_{\mathrm{inc}}^{\mathrm{spin}} + I_{\mathrm{inc}}^{\mathrm{isot}} + I_{\mathrm{coh}} + I_{\mathrm{magn}}^{v} \tag{6}$$

$$I_w^{\mathrm{SF}} = \tfrac{2}{3} I_{\mathrm{inc}}^{\mathrm{spin}} + 0 + 0 + I_{\mathrm{magn}}^{v} \tag{7}$$

$$I_w^{\mathrm{NSF}} = \tfrac{1}{3} I_{\mathrm{inc}}^{\mathrm{spin}} + I_{\mathrm{inc}}^{\mathrm{isot}} + I_{\mathrm{coh}} + I_{\mathrm{magn}}^{w}. \tag{8}$$

($\boldsymbol{P}$ and $\boldsymbol{Q}$: the direction of the incident neutron polarization and that of the scattering vector, respectively. 'spin'/'inc' = nuclear spin incoherent scattering, 'isot'/'inc' = nuclear isotope incoherent scattering, 'coh' = nuclear coherent (phonon) scattering, 'magn' = magnetic scattering with (squares of) matrix elements of u-, v-and w-components of the angular momentum operator in the instrumental coordinate system; for definitions, see figure 13.)

Before discussing the results, it should be noted that one has to distinguish, in principle, three coordinate systems: the instrumental (u, v, w), the crystalline (a, b, c) and the quantum mechanical (x, y, z) with quantization axis z, e.g., when considering certain sets of CF parameters. The correspondence between the instrumental and the crystalline system is shown in figure 12 for two different $\boldsymbol{Q}$-scans. By subtraction of equations (5) from (3), the v-component of the magnetic scattering can be obtained; subtraction of equations (7) from (3) yields the w-component.

By comparing the various components it was found that the intensity of the 23 meV CF transition is very anisotropic (figure 13) at 20 K. The $w(c)$-component is much stronger than the

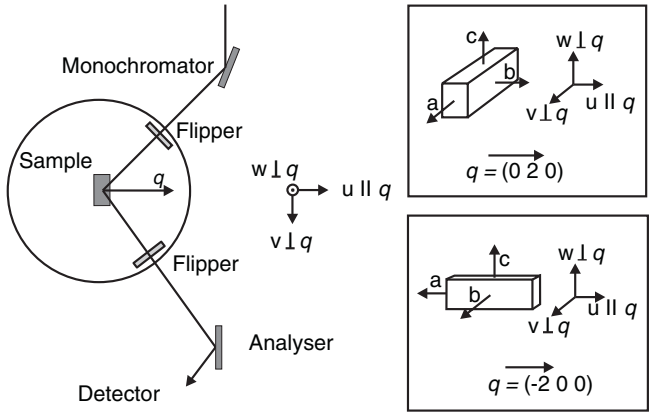

Figure 12. A schematic picture of the triple-axis spectrometer IN20 at the Institut Laue-Langevin. The experimental coordinate system (u, v, w) is shown. In the boxes (right), the sample orientation with respect to the experimental coordinate system can be seen for the experimental set-up for measuring at $\boldsymbol{Q} = (020)$ (top) and $(\bar{2}00)$ (bottom).

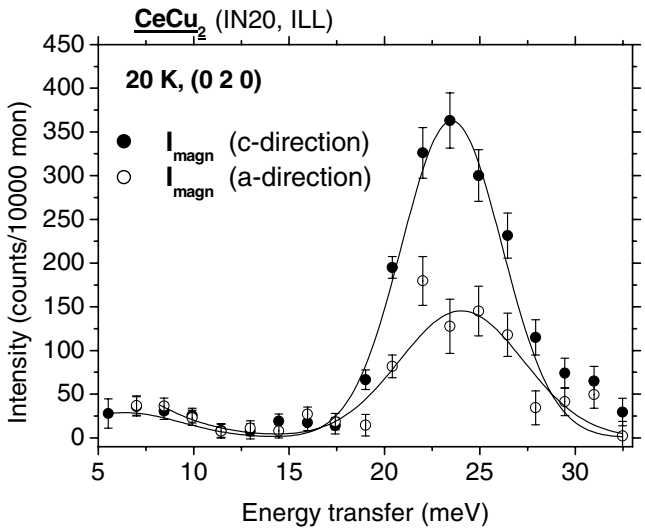

Figure 13. Comparison of the w- and v-components of the magnetic scattering, measured at $\boldsymbol{Q} = (020)$ and $T = 20$ K. For the CF transition at 23 meV the v-component of the magnetic scattering (in this orientation of the sample representing the a-component of the crystal) is much smaller than the w-component (the c-direction of the sample). The CF transition is very anisotropic.

$v(a)$-component. From that and from further measurements of the b-component, the matrix elements for the CF transition can be calculated. No magnetic intensity is found between 12 and 17 meV, only some weak intensity is observed below 10 meV, possibly from a small but non-zero matrix element for the transition from the ground state to the first excited state expected around 9 meV.

In figure 14 the results for the temperature-dependent measurements of the $w(c)$-component at $\boldsymbol{Q} = (020)$ can be seen. At 20 K the 23 meV CF transition is strong. For higher temperatures (200 and 400 K) the intensity of the 23 meV peak diminishes as expected. But

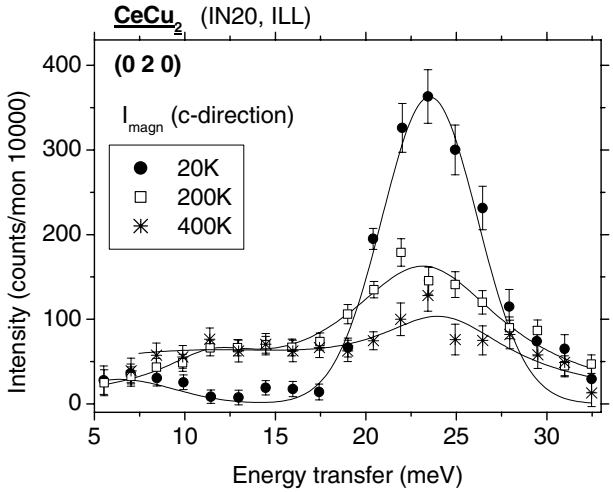

Figure 14. Comparison of the magnetic w-component (c-direction of the sample) of the $CeCu_2$ neutron spectrum. The data were obtained at IN20 at temperatures of 20, 200 and 400 K, measured at $\boldsymbol{Q} = (020)$. The peak at 23 meV represents the CF transition from the ground state to the second excited state. In the energy region between 10 and 17 meV for increased temperatures (data at 200 and 400 K) a broad peak can be observed, which is not visible at 20 K. It is due to the CF transition from the first to the second excited level, which is strongly broadened by the coupling to the phonons.

there is a remarkable rise of magnetic intensity in the energy range between 10 and 15 meV as was also observed in the 1T1 spectra. That confirms the assumption that this magnetic intensity is due to the CF transition from the first to the second excited level. It is strongly broadened by the coupling to certain phonons (with A_{1g} symmetry) that are found at energies between 7 and 17 meV. The additional broad magnetic intensity is observable only at temperatures above 100 K, when the first excited level becomes thermally populated.

5. Conclusions and outlook

In this article we have given an overview of experimental data obtained by inelastic neutron scattering experiments that indicate the existence of a strong coupling between lattice vibrations (phonons) and electronic excitations (CF transitions) in three selected compounds containing the rare-earth elements Ce and Yb: $CeAl_2$, $CeCu_2$ and $YbPO_4$. A necessary but not sufficient condition for the occurrence of such a dynamic coupling is that both the symmetries of the CF transitions and the energies involved coincide for the two subsystems.

A simple picture of the coupling may be as follows: the crystalline electric field (which determines the CF splitting and thus the CF transitions) is made up of the electric charges of the ions surrounding the rare-earth ion; it depends strongly on the exact atomic positions. Hence the CF interaction strength is modulated if the positions are (dynamically) changed by the lattice vibrations. To date, a detailed theoretical description has only been put forward for the situation found experimentally for $CeAl_2$: the so-called 'bound state between a phonon and a CF transition' as introduced by Thalmeier and Fulde [5].

The study of $CeCu_2$ has recently been complemented by investigations on the isostructural compounds YCu_2 and $NdCu_2$ [26]. The experiments on YCu_2 showed a negligible temperature dependence of the phonon energies. This is further evidence that the observed softening in

$CeCu_2$ (and $NdCu_2$) is indeed due to the CF–phonon interaction. Furthermore, a symmetry analysis showed that in $NdCu_2$ and $CeCu_2$ the only phonons that soften are those which transform at the Γ point according to the irreducible representation A_{1g}. According to a symmetry analysis of the CF–phonon interaction term in the Hamiltonian, only these phonons may couple to the CF.

However, still little is known about the magnitude of the CF–phonon interaction. A first quantitative estimation has been performed using the point charge model [26] and the findings agree well with the available data for $NdCu_2$. But this is only a partial description of the physics: in RCu_2 compounds the lattice is near an instability and the CF–phonon interaction may induce a structural phase transition in high magnetic fields [27, 28], the origin of which is still not understood.

It is possible that if the 4f electrons with a strong coupling to the lattice vibrations become delocalized by application of pressure, they may form heavy quasi-particles. If the strong coupling persists it may lead to superconductivity at low temperatures. Such a heavy-fermion superconductivity has been reported for $CeCu_2$ [29]. Understanding the origin and maximizing the CF–phonon interaction by means of further experimental and theoretical research might have an important impact on finding new heavy-fermion superconductors.

To give an example: measurements of phonon energies in high magnetic fields by INS, x-ray or optical spectroscopy could be used to determine the interaction strength. Complementary to these experiments, polarized neutron spectroscopy could measure the interaction by looking at the field and temperature dependence of the magnetic part of the spectrum. A theory of coupled systems needs to be developed which is applicable to all symmetries and allows a full treatment of the magnetic field and the neutron polarization.

Acknowledgment

This work was partly supported by Deutsche Forschungsgemeinschatt through Sonderforschungsbereich 463 (Seltenerd-Übergangsmetallverbindungen: Struktur, Magnetismus und Transport).

References

[1] Dörfler W and Schaack G 1985 *Z. Phys.* B **59** 283
[2] Becker P C, Williams G M, Edelstein N M, Koningstein J A, Boatner L A and Abraham M M 1992 *Phys. Rev.* B **45** 5027
[3] Loewenhaupt M, Rainford B D and Steglich F 1979 *Phys. Rev. Lett.* **42** 1709
[4] Reichardt W and Nücker N 1984 *J. Phys. F: Met. Phys.* **14** L135
[5] Thalmeier P and Fulde P 1982 *Phys. Rev. Lett.* **49** 1588
[6] Thalmeier P 1984 *J. Phys. C: Solid State Phys.* **17** 4153
[7] Loewenhaupt M, Reichardt W, Pynn R and Lindley E 1987 *J. Magn. Magn. Mater.* **63/64** 73
[8] Loewenhaupt M and Reichardt W 1984 *ILL Report on Experiment* 4-03-332
[9] Lüthi B and Lingner C 1979 *Z. Phys.* B **34** 157
[10] Schiltz R J and Smith J F 1974 *J. Appl. Phys.* **45** 4681
[11] Yeh C T, Reichardt W, Renker B, Nücker N and Loewenhaupt M 1981 *J. Physique* **42** C6 371
[12] Cullen J R and Clark A E 1977 *Phys. Rev.* B **15** 4510
[13] Loong C-K, Loewenhaupt M, Nipko J C, Braden M, Reichardt W and Boatner L A 1999 *Phys. Rev.* B **60** R12549
[14] Harley R T 1987 *Spectroscopy of Solids containing Rare Earth Ions* ed A A Kaplyanskii and R M Macfarlane (Amsterdam: Elsevier) p 557
[15] Gehring G A and Gehring K A 1975 *Rep. Prog. Phys.* **38** 1
[16] Nipko J, Grimsditch M, Loong C-K, Kern S, Abraham M M and Boatner L A 1996 *Phys. Rev.* B **53** 2286
[17] Nipko J C, Loong C-K, Loewenhaupt M, Braden M, Reichardt W and Boatner L A 1997 *Phys. Rev.* B **56** 11584
[18] Loong C-K, Soderholm L, Goodman G L, Abraham M M and Boatner L A 1993 *Phys. Rev.* B **48** 6124

[19] Loong C-K, Soderholm L, Abraham M M, Boatner L A and Edelstein N M 1993 *J. Chem. Phys.* **98** 4214
[20] Yamada Y 1977 *Electron–Phonon Interactions and Phase Transitions* ed T Riste (New York: Plenum) p 370
[21] Sinha S K 1977 *Int. Conf. on Lattice Dynamics* ed M Balkanski (Paris: Flammarion Sciences) p 7
[22] Loewenhaupt M, Prager M, Gratz E and Frick B 1988 *J. Magn. Magn. Mater.* **76/77** 415
[23] Loewenhaupt M, Gratz E, Pillmayr N and Müller H 1990 *Physica* B **163** 427
[24] Loewenhaupt M, Witte U, Kramp S, Braden M and Svoboda P 2002 *Physica* B **312/313** 181
[25] Schedler F, Witte U, Loewenhaupt M and Kulda J 2002 *Physica* B at press
[26] Hense K 2002 CEF–phonon interaction in the orthorhombic compound $NdCu_2$ *Thesis* Technische Universität Wien
[27] Hashimoto Y, Kindo K, Takeuchi T, Senda K, Date M and Yamagishi A 1994 *Phys. Rev. Lett.* **72** 1922
[28] Kramp S, Doerr M, Rotter M, Loewenhaupt M and van der Kamp R 2000 *Eur. Phys. J.* B **18** 559
[29] Vargoz E, Link P and Jaccard D 1997 *Physica* B **230–232** 182